Journal of *Marine Science and Engineering*

MDPI

Article

Interaction of a Flexural-Gravity Wave with a Vertical Rigid Plate Built in a Floating Elastic Plate

Qiyuan Wu [1], Tatyana Khabakhpasheva [2,*] and Baoyu Ni [1] and Alexander Korobkin [2]

[1] College of Shipbuilding Engineering, Harbin Engineering University, Harbin 150001, China
[2] School of Mathematics, University of East Anglia, Norwich NR4 7TJ, UK
* Correspondence: t.khabakhpasheva@uea.ac.uk

Abstract: The linear two-dimensional problem of interaction between an hydroelastic wave propagating along an elastic floating ice plate with built-in vertical rigid plate is studied. The fluid under the ice is inviscid and incompressible. The fluid depth is finite. The deflection of the ice plate is described by the linear theory of thin elastic plates. The flow under the ice is potential. The total velocity potential is decomposed into the potential of the incident wave, even potential caused by the vertical motion of the rigid plate, and an odd potential caused by the rotation of the rigid plate. The vertical mode method is used. The third potential is obtained by solving a mixed boundary-value problem numerically using Chebyshev polynomials. The solution is validated by analysis of its convergence. The first and second potentials, and the corresponding deflections and strains of the ice plate, are obtained analytically. The motions of the rigid plate, as well as deflection and strains in the floating plate, are numerically analyzed. It is shown that the rotation of the rigid plate due to the incident wave is the main factor of increasing strains in the ice plate.

Keywords: hydroelasticity; flexural-gravity wave; floating ice plate; interaction; vertical mode method; strains; deflections

Citation: Wu, Q.; Khabakhpasheva, T.; Ni, B.; Korobkin, A. Interaction of a Flexural-Gravity Wave with a Vertical Rigid Plate Built in a Floating Elastic Plate. *J. Mar. Sci. Eng.* **2023**, *11*, 697. https://doi.org/10.3390/jmse11040697

Academic Editor: Majid Mohammadian

Received: 31 January 2023
Revised: 19 March 2023
Accepted: 21 March 2023
Published: 24 March 2023

1. Introduction

Wave propagating under sea ice cover has been studied intensively for several decades. The importance of this topic has been increasing year by year as the ice reduction accelerates in the polar regions. Thanks to the global temperature rising, sea ice can be found further from the pole, and a chance of shipping through the ice-covered regions increases. New commercial routes through the Arctic can significantly reduce the shipping time and improve its economic efficiency. On the other hand, the amount of natural resources in the polar regions is vast. Gautier et al. [1] wrote "the United States Geological Survey has assessed the area north of the Arctic Circle and concluded that about 30% of the world's undiscovered gas and 13% of the world's undiscovered oil may be found there, mostly offshore under less than 500 meters of water. Undiscovered natural gas is three times more abundant than oil in the Arctic and is largely concentrated in Russia." The potential of renewable energy, such as solar and wind energies, in the polar regions is too important to be ignored. The economic needs in the polar region have attracted more attention to modeling sea ice.

Modeling sea ice and waves propagating in ice-covered waters is challenging because the properties of the ice change significantly from place to place, see [2–6]. They depend on air temperature, water salinity, and how the ice was built up. This makes it difficult to construct a stable and reliable sea ice mechanical model. However, modeling the ice cover as a thin floating elastic plate of constant thickness proved to be a reasonable approach to practical problems with relatively long waves, see [7]. The ice/water interaction problems become more complicated in the presence of other structures in either water or on ice, or in both of them. Flexural-gravity waves diffracted by vertical cylinders frozen in ice were

studied in [8–12]. Waves propagating in an ice channel with vertical walls are investigated in [13–17]. In all of these studies, the structural motion was not included.

Problems of flexural-gravity wave interaction with a free moving structure are more complicated. Such problems are coupled: deflection of the floating ice plate, flow under the ice, and the motions of the structure should be determined at the same time. A vertical rigid plate built-in a floating ice sheet could be the simplest model of ice/water/structure interaction. This problem is investigated in the present paper using the vertical mode method [8,9,11,12] for water of finite depth. There are parts of the rigid plate below the ice in water and above the ice. The part of the rigid plate above the ice does not participate in interaction with water, but it changes the mass of the plate and its moment of inertia. The thickness of the plate is assumed to be small, which simplifies the analysis and makes it possible to separate the vertical motion of the plate and the plate rotation. The rigid plate motions are caused by a linear incident wave and are governed by equations of mechanics. A similar problem was considered recently in [18] but for infinite water depth, where the vertical mode method is not applicable, and for elastic vertical plate.

The approach of the present paper is to divide the original problem in parts, which are easier to solve and validate, and finally combine all of the obtained solutions to arrive at the complete solution of the original problem. The finite depth of the liquid under the floating elastic plate makes it possible to use the so-called vertical modes to represent the velocity potential. The vertical modes accommodate the complex boundary conditions at the elastic plate. Integral transforms also can be used to this aim, see [10], but they provide the same result as the vertical mode method as it was proved in [9]. To find the odd part of the velocity potential, the solution of a mixed boundary-value problem is required. This is a challenging problem, which is solved by using the Chebyshev polynomials.

This paper aims to provide a theoretical basis for subsequent research on a floating elastic plate with several built-in vertical plates. The structure of the paper is organized as follows. The formulation of the problem is given in Section 2. The vertical mode method is applied to solve the problem in Section 3. Numerical algorithms are described in Section 4. Numerical results are presented in Section 5. Conclusions and future work are discussed in Section 6.

2. Formulation of the Problem

The two-dimensional linear problem of a flexural-gravity wave interacting with a rigid vertical plate built in a floating ice sheet is studied, see Figure 1. The ice sheet is considered as an infinite thin elastic plate of constant thickness h. The density of the ice is ρ_{ice}, and the ice rigidity is $D = Eh^3/[12(1-\nu^2)]$, where E and ν are the Young's modulus and Poisson's ratio of the ice respectively. The liquid under the ice is inviscid, incompressible, and of finite depth H. The rigid plate built-in the ice sheet is of length L under the ice and of length ℓ above the ice, of negligible thickness, and of mass m_0, and the moment of inertia J_0 with respect to the point is where the rigid plate is in contact with the ice sheet. This point is taken as the origin of the Cartesian coordinate system Oxy, see Figure 1. The ice/liquid interface corresponds to the line $y = 0$ at equilibrium without any motions of the ice plate and any flow under the plate. The line $y = -H$ corresponds to the bottom of the flow region. Note that $L \leq H$. The liquid flow caused by the ice plate deflection and the rigid plate motions is assumed potential. The flow region Ω within the linear potential theory is the the strip $-H < y < 0$ with the cut $x = 0$, $-L < y < 0$, which corresponds to the submerged part of the rigid plate at equilibrium. The flow region is independent of time within the linear approximation. This is the coupled problem of linear hydroelasticity, where the plate deflection $y = W(x,t)$; t is the time; the flow under the ice is described by a velocity potential $\Phi(x,y,t)$; and the motions of the rigid plate should be determined at the same time.

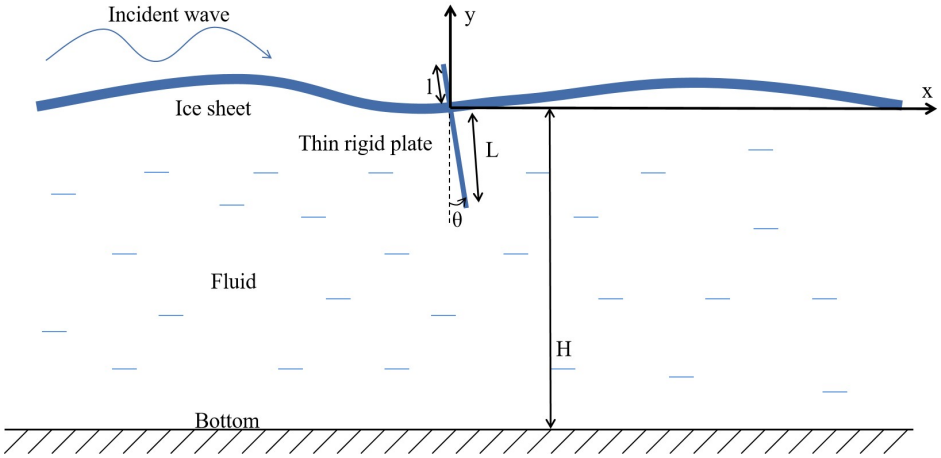

Figure 1. Sketch of wave propagating in an ice sheet with a rigid plate.

The incident flexural-gravity wave, $W_{inc}(x,t) = a_i \cos(k_0 x - \omega t)$, is of small amplitude a_i with a frequency ω and wavenumber k_0, where ω and k_0 are related by the dispersion relation [7],

$$\omega^2(\rho_{ice}h + \frac{\rho}{k_0 \tanh(k_0 H)}) = \rho g + D k_0^4, \tag{1}$$

ρ is the liquid density, g is the gravitational acceleration, and $\omega > 0, k_0 > 0$. The velocity potential of the incident wave is given by

$$\Phi_{inc}(x,y,t) = a_i \omega \frac{\cosh[k_0(y+H)]}{k_0 \sinh(k_0 H)} \sin(k_0 x - \omega t). \tag{2}$$

The linear theory of hydroelasticity is applicable if the wave slope, $a_i k_0$, is small. The floating ice plate can be treated as a thin elastic plate if the plate thickness h is much smaller than the incident wave length $2\pi/k_0$, which provides the condition $k_0 h \ll 1$.

Note that the deflection $W(x,t)$ is continuous together with its first derivatives at $x = 0$, but the second and third derivatives, $W_{xx}(x,t)$ and $W_{xxx}(x,t)$, are, in general, discontinuous at the place of the rigid plate, $x = 0$. It is convenient to write the thin plate equation separately for the right, $x > 0$, and the left, $x < 0$, parts,

$$\rho_{ice} h \frac{\partial^2 W}{\partial t^2} + D \frac{\partial^4 W}{\partial x^4} = P(x,0,t) \quad (-\infty < x < 0, 0 < x < +\infty, y = 0), \tag{3}$$

where $P(x,0,t)$ is the hydrodynamic pressure on the ice/liquid interface, which is given by the linearised Bernoulli equation

$$P(x,0,t) = -\rho \frac{\partial \Phi}{\partial t}(x,0,t) - \rho g W(x,t). \tag{4}$$

The plate deflection in the far field on the left from the rigid plate behaves as

$$W(x,t) = a_i \cos(k_0 x - \omega t) + a_R \cos(-k_0 x - \omega t + \delta_R) + o(1) \quad (x \to -\infty), \tag{5}$$

and in the far field on the right from the rigid plate as

$$W(x,t) = a_T \cos(k_0 x - \omega t + \delta_T) + o(1) \quad (x \to \infty), \tag{6}$$

where $o(1)$ stands for terms decaying exponentially as $|x| \to \infty$, a_R and a_T are the amplitudes and δ_R and δ_T are the phase shifts of the reflected and transmitted flexural-gravity waves correspondingly. The values of a_R, a_T, δ_R, and δ_T are to be determined as part of the solution.

The velocity potential $\Phi(x, y, t)$ satisfies the Laplace equation in the flow region,

$$\nabla^2\Phi = 0 \quad ((x, y) \in \Omega), \tag{7}$$

the boundary conditions on the bottom,

$$\frac{\partial\Phi}{\partial y} = 0 \quad (y = -H), \tag{8}$$

the linearized kinematic boundary condition on the ice/liquid interface,

$$\frac{\partial\Phi}{\partial y} = \frac{\partial W}{\partial t}(x, t) \quad (y = 0), \tag{9}$$

and the conditions on the right, $x = +0$, and left, $x = -0$, surfaces of the moving rigid plate,

$$\frac{\partial\Phi}{\partial x}(0^{\pm}, y, t) = -y\frac{\mathrm{d}\theta(t)}{\mathrm{d}t} \quad (-L < y < 0), \tag{10}$$

where $\theta(t)$ is the inclination angle of the rigid plate; $\theta = 0$ at equilibrium; when the rigid plate is vertical, θ is positive anticlockwise, see Figure 1. The behavior of the velocity potential as $x \to \pm\infty$ follows from (5) and (6) in a similar way as (2) follows from the form of the incident deflection wave.

The time-dependent vertical displacement $\eta(t)$ and inclination angle $\theta(t)$ of the rigid plate are governed by equations,

$$m_0\frac{\mathrm{d}^2\eta(t)}{\mathrm{d}t^2} = N_s(0^-, t) - N_s(0^+, t), \tag{11}$$

$$J_0\frac{\mathrm{d}^2\theta(t)}{\mathrm{d}t^2} = [M_s(0^+, t) - M_s(0^-, t)] + [M_f(0^+, t) - M_f(0^-, t)], \tag{12}$$

where $M(x, t)$, $N(x, t)$ are the bending moment and shear force, respectively; subscript s stands for solid (ice); subscript f stands for fluid; and m_0 and J_0 are the mass and the moment of inertia of the rigid plate per unit width, respectively. A rigid plate, which is of length L below the floating elastic plate and ℓ above the the floating plate, is of mass $m_0 = \rho_r h_r(L + \ell)$, where ρ_r is the density of the rigid plate material and h_r is the rigid plate thickness. The moment of inertia of such a plate is $J_0 = \frac{1}{3}m_0(L^3 + \ell^3)/(L + \ell)$.

The bending moment and shear force in the ice plate are proportional to the second and third derivatives of the deflection $W(x, t)$ with respect to x,

$$M_s = D\frac{\partial^2 W}{\partial x^2}\ ,\ N_s = D\frac{\partial^3 W}{\partial x^3}. \tag{13}$$

The hydrodynamic moments acting on the submerged part of the rigid plate are given by

$$M_f(0^{\pm}, t) = -\rho\frac{\mathrm{d}}{\mathrm{d}t}\int_{-L}^{0}\Phi(0^{\pm}, y, t)y\,\mathrm{d}y \tag{14}$$

within the linear theory. At the connection point between the floating elastic plate and the rigid plate, we have

$$\eta(t) = W(0^+, t) = W(0^-, t), \quad \theta(t) = \frac{\partial W}{\partial x}(0^+, t) = \frac{\partial W}{\partial x}(0^-, t). \tag{15}$$

No initial conditions are required for the formulated problem (1)–(15). We shall determine the time-periodic solution of this problem.

The velocity potential $\Phi(x, y, t)$, the plate deflection $W(x, t)$, the vertical displacement of the rigid plate $\eta(t)$, and the inclination angle of the rigid plate $\theta(t)$ are sought in the form

$$W(x,t) = \Re(w(x)e^{-i\omega t}), \quad \Phi(x,y,t) = \Re(-i\omega\phi(x,y)e^{-i\omega t}),$$
$$\eta(t) = \Re(\eta_a e^{-i\omega t}), \quad \theta(t) = \Re(\theta_a e^{-i\omega t}), \tag{16}$$

where $w(x)$ and $\phi(x,y)$ are complex-valued functions, η_a and θ_a are complex numbers to be determined, and $\Re$ stands for the real part of a complex number. The complex plate deflection $w(x)$ and the velocity potential $\phi(x,y)$ are convenient to decompose as

$$w(x) = w_{inc}(x) + w_o(x) + w_e(x), \quad \phi(x,y) = \phi_{inc}(x,y) + \phi_o(x,y) + \phi_e(x,y), \tag{17}$$

where $w_{inc}(x)$ and $\phi_{inc}(x,y)$ correspond to the incident wave,

$$w_{inc}(x) = a_i e^{ik_0 x}, \quad \phi_{inc}(x,y) = a_i \frac{\cosh[k_0(y+H)]}{k_0 \sinh(k_0 H)} e^{ik_0 x}, \tag{18}$$

$w_o(x)$ and $\phi_o(x,y)$ are unknown odd with respect to x functions, $w_o(-x) = -w_o(x)$, and $w_e(x)$ and $\phi_e(x,y)$ are unknown even with respect to x functions, $w_e(-x) = w_e(x)$. Only the right-hand side of the flow region, $x > 0$, can be considered from now on. In particular, the matching conditions (15) read now as

$$\eta_a = a_i + w_e(0), \quad \theta_a = ik_0 a_i + w_0'(0), \tag{19}$$

where a prime stands for derivative with respect to x. The deflections $w_o(x)$ and $w_e(x)$ describe outgoing waves in the far field,

$$w_o(x) = A_o e^{ik_0 x} + o(1), \quad w_e(x) = A_e e^{ik_0 x} + o(1) \quad (x \to +\infty), \tag{20}$$

where the complex amplitudes A_o and A_e are to be determined. Equations (5), (6), (17), and (20) provide the parameters of the radiated and transmitted waves as

$$a_T e^{i\delta_T} = a_i + A_e + A_o, \quad a_R e^{i\delta_R} = A_e - A_o. \tag{21}$$

The equations and boundary conditions in the formulated problem (1)–(15), which are satisfied in the right part of the flow region, $x > 0$, are valid for the odd and even components of the solution separately. Using $*$ for either o or e, we find

$$\nabla^2 \phi_* = 0 \quad (x > 0, -H < y < 0), \tag{22}$$

$$\frac{\partial \phi_*}{\partial y} = 0 \quad (x > 0, y = -H), \tag{23}$$

$$\frac{\partial \phi_*}{\partial y} = w_*(x) \quad (x > 0, y = 0), \tag{24}$$

$$D\frac{\mathrm{d}^4 w_*}{\mathrm{d}x^4} + (\rho g - \rho_{ice} h\omega^2) w_* = \rho\omega^2 \phi_*(x,0) \quad (x > 0). \tag{25}$$

The conditions at $x = +0$ have different forms for odd,

$$w_e'(0) = 0, \tag{26}$$

$$2Dw_e'''(0) - m_0\omega^2 w_e(0) = m_0 a_i \omega^2, \tag{27}$$

$$\frac{\partial \phi_e}{\partial x}(0,y) = 0 \quad (-H < y < 0), \tag{28}$$

and even components,

$$w_o(0) = 0, \tag{29}$$

$$2Dw_o''(0) + J_0\omega^2 w_o'(0) = -2\rho\omega^2 \int_{-L}^{0} \phi_o(0,y) y \mathrm{d}y - i a_i k_0 J_0 \omega^2, \tag{30}$$

$$\phi_o(0,y) = 0 \quad (-H < y < -L), \tag{31}$$

$$\frac{\partial \phi_o}{\partial x}(0,y) = -iya_i k_0 - yw_o'(0) - ia_i \frac{\cosh[k_0(y+H)]}{\sinh(k_0 H)} \quad (-L < y < 0). \tag{32}$$

The conditions (26)–(28) for the even component of the solution imply that there is no flow through $x = 0$, the slope of the floating plate at this edge is zero, and the edge is connected to the bottom with a spring, see section 7 in [19], with the vertical forcing applied to the edge. The conditions (29)–(32) for the odd component of the solution imply that the plate edge does not move vertically but can rotate subject to the restoring force and the forcing caused by the incident wave and the hydrodynamic pressure acting on the submerged part of the rigid plate, see [20]. The far-field conditions (20) should also be satisfied, where the complex amplitudes A_o and A_e are to be determined. These amplitudes and the unknown functions $w_o(x)$, $\phi_o(x,y)$ and $w_e(x)$, $\phi_e(x,y)$ are proportional to the amplitude of the incident wave a_i, which can be set unity in the analysis and returned back in the final solution as the factor.

The ratio of amplitude of the reflected wave a_R to the amplitude of the incident wave a_i is known as the reflection coefficient R, and the ratio of amplitude of the transmitted wave a_T to the amplitude of the incident wave a_i is known as the transmission coefficient T. We shall investigate these coefficients depending on the wave frequency and parameters of the problem. The distribution of the deflection amplitude $|w(x)|$ will be studied with focus on the maximum amplitude depending on parameters of the rigid plate. The time-periodic strains in the elastic plate are given by the formula

$$E(x,t) = \Re(\varepsilon(x)e^{-i\omega t}), \quad \varepsilon(x) = \frac{h}{2}\frac{\mathrm{d}^2 w}{\mathrm{d}x^2}, \quad \varepsilon_{\max} = \max_{x \geq 0} |\varepsilon(x)|. \tag{33}$$

We are concerned with $\varepsilon_{\max}$ depending on the parameters of the problem.

3. Solution of the Problem by the Vertical Mode Method

Note that the odd and even components of the solution are independent of one another and are calculated independently. Both components are obtained by the so-called vertical mode method. The vertical modes of a floating elastic plate were introduced in [21,22], applied to two-dimensional problems in [23,24], and applied to three-dimensional problems in [8,9]. For liquid of depth H, the vertical modes are given by

$$f_n(y) = \frac{\cosh[k_n(y+H)]}{k_n \sinh[k_n H]}, \tag{34}$$

where k_n are the complex roots of the dispersion Equation (1) with positive imaginary parts. These roots include real positive root k_0, two complex roots $k_{-2} = (-a+ib)/H$, $k_{-1} = (a+ib)/H$, where $a > 0$, $b > 0$, and infinite numbers of pure imaginary roots $k_n = i\mu_n$, $\mu_{n+1} > \mu_n > 0$ for $n \geq 1$. The modes satisfy the equations

$$f_n'' - k_n^2 f_n = 0 \quad (-H < y < 0), \tag{35}$$

$$f_n'(-H) = 0, \quad D\frac{\mathrm{d}^5 f_n}{\mathrm{d}y^5}(0) + (\rho g - \rho_{ice} h\omega^2)\frac{\mathrm{d}f_n}{\mathrm{d}y}(0) = \rho\omega^2 f_n(0), \tag{36}$$

and $f_n'(0) = 1$. The modes are orthogonal in the following sense,

$$\langle f_n(y), f_m(y)\rangle = 0 \quad (n \neq m), \quad \langle f_n(y), f_n(y)\rangle = Q_n \quad (n \geq -2), \tag{37}$$

where the scalar product is defined by

$$\langle F_1(y), F_2(y)\rangle = \int_{-H}^{0} F_1(y)F_2(y)\,\mathrm{d}y + \frac{D}{\rho\omega^2}(F_1'''(0)F_2'(0) + F_1'(0)F_2'''(0)), \tag{38}$$

for any two functions $F_1(y)$ and $F_2(y)$ defined in the interval $-H < y < 0$, and

$$Q_n = \frac{H^3}{2\kappa_n^2 q^2}\Big[(\kappa_n^4+\delta)^2\kappa_n^2 + q(5\kappa_n^4+\delta-q)\Big], \tag{39}$$

$\kappa_n = k_n H$ is the dimensionless wavenumber, $q = \rho\omega^2 H^5/D$, and $\delta = (\rho g - \rho_{ice} h\omega^2)H^4/D$. The dispersion relation (1) written with respect to dimensionless wavenumber κ reads $(\kappa^4+\delta)\kappa\tanh\kappa = q$. Equations (38) and (39) are similar to Equations (32) and (33) from [9] but written in the dimensional variables.

The products $e^{ik_n x}f_n(y)$ satisfy Equations (22)–(25) and decay as $x \to +\infty$ except for $n = 0$. The product $e^{ik_o x}f_0(y)$, where k_0 is real and positive, describes a wave propagating towards $x = +\infty$. Therefore, a general solution of the boundary-value problem (20), (22)–(25) is given by a superposition,

$$\phi_*(x,y) = \sum_{n=-2}^{\infty} A_n^* e^{ik_n x}f_n(y), \quad w_*(x) = \sum_{n=-2}^{\infty} A_n^* e^{ik_n x}, \tag{40}$$

with undetermined coefficients A_n^*, where $*$ stands either for o (odd component of the solution) or e (even component of the solution). These coefficients and the complex amplitudes A_o and A_e in (20) are obtained using the conditions (26)–(32) at $x = 0$. Equations (20) and (40) provide $A_0^o = A_o$ and $A_0^e = A_e$.

3.1. Even Component of the Plate Deflection

We calculate the following limit for $m \geq -2$ in two ways, by using (40) and (37), where $*$ is changed to e, and by using the definition (38) of the scalar product,

$$\lim_{x\to 0}\langle\frac{\partial\phi_e(x,y)}{\partial x}, f_m(y)\rangle = \lim_{x\to 0}\langle\sum_{n=-2}^{\infty} A_n^e ik_n e^{ik_n x}f_n(y), f_m(y)\rangle = A_m^e ik_m Q_m, \tag{41}$$

$$\lim_{x\to 0}\langle\frac{\partial\phi_e(x,y)}{\partial x}, f_m(y)\rangle =$$

$$= \lim_{x\to 0}\Big[\int_{-H}^{0}\frac{\partial\phi_e}{\partial x}(x,y)f_m(y)\mathrm{d}y + \frac{D}{\rho\omega^2}(-w_e'''(x)f_m'(0) + w_e'(x)f_m'''(0))\Big] =$$

$$= \frac{-Dw_e'''(0)}{\rho\omega^2} = -\frac{m_0}{2\rho}(a_i + w_e(0)). \tag{42}$$

In (42), conditions (26)–(28) and equalities

$$\frac{\partial^3(\partial\phi_e/\partial x)}{\partial y^3}(x,0) = \frac{\partial^2(\partial^2\phi_e)/\partial x\partial y)}{\partial y^2}(x,0) = -\frac{\partial^3(\partial\phi_e/\partial y)}{\partial x^3}(x,0) = -w_e'''(x),$$

$$\frac{\partial^2\phi_e}{\partial x\partial y} = w_e'(x)$$

were used. Equating the right-hand sides in (41) and (42), we obtain the formula for the coefficients A_m^e, where $m \geq -2$,

$$A_m^e = \frac{im_0}{2\rho k_m Q_m}(a_i + w_e(0)). \tag{43}$$

The unknown deflection $w_e(0)$ at $x = 0$ is obtained by substituting (43) in (40), setting $x = 0$, and resolving the result with respect to $w_e(0)$,

$$w_e(0) = a_i\frac{\gamma}{1-\gamma}, \qquad \gamma = \frac{im_0}{2\rho}\sum_{n=-2}^{\infty}\frac{1}{k_n Q_n}. \tag{44}$$

Equations (44), (43), and (40) provide the even component of the elastic plate deflection,

$$w_e(x) = \frac{ia_i m_0}{2\rho(1-\gamma)} \sum_{n=-2}^{\infty} \frac{e^{ik_n x}}{k_n Q_n}. \tag{45}$$

The even component of the strain in the plate follows from (33) as

$$\varepsilon_e(x) = \frac{-ia_i m_0 h}{4\rho(1-\gamma)} \sum_{n=-2}^{\infty} \frac{k_n e^{ik_n x}}{Q_n}. \tag{46}$$

The complex amplitude of the radiated wave A_e in (20) is given by

$$A_e = A_0^e = \frac{ia_i m_0}{2\rho(1-\gamma)k_0 Q_0}. \tag{47}$$

It is shown in [9] that $Q_n = O(n^8)$ as $n \to \infty$. Therefore, the series in (44), (45), and (46) converge quickly. There is no even component of the solution if the mass of the rigid plate m_0 is negligible.

3.2. Odd Component of the Plate Deflection

The odd component is calculated in the same way as the even component in section 3.1. The solution is sought in the form (40), (34), where $*$ is changed to o. It is convenient to introduce the unknown derivative $(\partial\phi_o/\partial x)(0,y) = u(y)$, on the vertical interval $-H < y < -L$. This derivative is determined using the condition (31). Note that the new unknown function $u(y)$ is square-root singular at $y = -L$ and $u'(-H) = 0$ to match the boundary condition at the bottom $y = -H$. We introduce a new variable $\xi = (y+H)/(H-L)$ for the interval $(-H, -L)$, where $0 < \xi < 1$, and search the function $u[y(\xi)]$ as the series

$$u[y(\xi)] = \frac{1}{\sqrt{1-\xi^2}} \sum_{k=0}^{\infty} u_k T_{2k}(\xi), \tag{48}$$

where $T_{2k}(\xi)$ are the even Chebyshev polynomials of the first kind and degree $2k$. The limits (41) and (42), where $m \geq -2$, calculated now for $\phi_0(x,y)$ provide

$$\lim_{x\to 0} \left\langle \frac{\partial\phi_o(x,y)}{\partial x}, f_m(y) \right\rangle = A_m^o i k_m Q_m, \tag{49}$$

$$\lim_{x\to 0} \left\langle \frac{\partial\phi_o(x,y)}{\partial x}, f_m(y) \right\rangle = -(ia_i k_0 + w_o'(0)) \int_{-L}^{0} y f_m(y)\mathrm{d}y - ia_i k_0 \int_{-L}^{0} f_0(y) f_m(y)\mathrm{d}y + \int_{-H}^{-L} u(y) f_m(y)\,\mathrm{d}y + \frac{D}{\rho\omega^2}(k_m^2 w_o'(0) - w_o'''(0)). \tag{50}$$

The integrals in (50) are denoted as P_m, $P_m^{(0)}$, and $P_m^{(G)}$, correspondingly. Multiplying Equation (35) by $f_0(y)$ and y, and integrating the results with respect to y from $-L$ to 0 by parts, we obtain

$$P_m = \frac{L f_m'(-L) + f_m(-L) - f_m(0)}{k_m^2}, \quad P_m^{(0)} = \frac{f_0(0) - f_m(0) + [f_0' f_m - f_0 f_m'](-L)}{k_m^2 - k_0^2}. \tag{51}$$

The series (48) provides

$$P_m^{(G)} = \sum_{k=0}^{\infty} u_k G_{mk}, \quad G_{mk} = \frac{H-L}{k_m \sinh[k_m H]} \int_0^1 T_{2k}(\xi) \cosh[k_m(H-L)\xi] \frac{\mathrm{d}\xi}{\sqrt{1-\xi^2}}. \tag{52}$$

The coefficients G_{mk} can be presented using the dimensionless wavenumber $\kappa_m = k_m H$, the parameter $\tilde{L} = L/H$, and the dispersion relation through the modified Bessel functions of complex arguments,

$$G_{mk} = \frac{\pi H^2 (1-\tilde{L})(\kappa_m^4 + \delta)}{2q \cosh[\kappa_m]} I_{2k}(\kappa_m(1-\tilde{L})), \tag{53}$$

where $I_{2k}(z)$ are the modified Bessel functions of the first kind and order $2k$.

Equating (49) and (50), we find

$$A_m^o = -a_i k_0 \frac{P_m + P_m^{(0)}}{k_m Q_m} + \frac{ik_m}{Q_m}\Big(\frac{P_m}{k_m^2} - \frac{D}{\rho\omega^2}\Big) w_o'(0) + \frac{iD}{\rho\omega^2 k_m Q_m} w_0'''(0) + \frac{P_m^{(G)}}{ik_m Q_m}, \tag{54}$$

where $w_o'(0)$, $w_0'''(0)$, and $P_m^{(G)}$ are to be determined using the conditions (29), (30) and (31).

The condition (31) and the series (40) provide

$$0 = \phi_o(0, y(\xi)) = \sum_{n=-2}^{\infty} A_n^o f_n[y(\xi)] \quad (0 < \xi < 1). \tag{55}$$

Multiplying both sides of this equation by $T_{2m}(\xi)/\sqrt{1-\xi^2}$, where $m \geq 0$, and integrating with respect to ξ from 0 to 1, we find

$$\sum_{n=-2}^{\infty} A_n^o G_{nm} = 0,$$

which yields the following system for the coefficients u_k using (54) and (52)

$$\sum_{k=0}^{\infty} u_k S_{km} = \frac{D}{\rho\omega^2} w_o'''(0) F_m^{(3)} + w_o'(0) F_m^{(1)} + i a_i k_0 F_m^{(0)}, \tag{56}$$

$$S_{km} = \sum_{n=-2}^{\infty} \frac{G_{nk} G_{nm}}{k_n Q_n}, \qquad F_m^{(0)} = \sum_{n=-2}^{\infty} \frac{(P_n + P_n^{(0)}) G_{nm}}{k_n Q_n},$$

$$F_m^{(1)} = \sum_{n=-2}^{\infty} \frac{P_n G_{nm}}{k_n Q_n} - \frac{D}{\rho\omega^2} \sum_{n=-2}^{\infty} \frac{k_n G_{nm}}{Q_n}, \qquad F_m^{(3)} = \sum_{n=-2}^{\infty} \frac{G_{nm}}{k_n Q_n}.$$

It is seen that $G_{nk} = O(n^{\frac{7}{2}})$ as $n \to \infty$. It can be shown that P_n and $P_n^{(0)}$ are of order $O(n^3)$ as $n \to \infty$. Therefore, the series for S_{km}, $F_m^{(0)}$ and $F_m^{(1)}$ converge slowly and should be evaluated with care.

The solution of the system reads

$$u_k = \frac{D}{\rho\omega^2} w_o'''(0) u_k^{(3)} + w_o'(0) u_k^{(1)} + i a_i k_0 u_k^{(0)}, \tag{57}$$

where $u_k^{(j)}$, $j = 0, 1, 3$ are solutions of the systems

$$\sum_{k=0}^{\infty} u_k^{(j)} S_{km} = F_m^{(j)}.$$

Substituting (57) in (52) and (54), one finds the coefficients A_m^o through two unknown, $w_0'(0)$ and $w_0'''(0)$,

$$A_m^o = \frac{a_i k_0}{k_m Q_m} B_m^{(0)} + \frac{ik_m}{Q_m} w_o'(0) B_m^{(1)} + \frac{iD}{\rho\omega^2 k_m Q_m} w_0'''(0) B_m^{(3)}, \tag{58}$$

$$B_m^{(0)} = -P_m - P_m^{(0)} + \sum_{k=0}^{\infty} u_k^{(0)} G_{mk},$$

$$B_m^{(1)} = \frac{P_m}{k_m^2} - \frac{D}{\rho\omega^2} - \frac{1}{k_m^2} \sum_{k=0}^{\infty} u_k^{(1)} G_{mk},$$

$$B_m^{(3)} = 1 - \sum_{k=0}^{\infty} u_k^{(3)} G_{mk}.$$

The conditions (29), (30), and the series (40) provide two equations with respect to $w_0'(0)$ and $w_0'''(0)$,

$$w_0'(0) \sum_{n=-2}^{\infty} \frac{k_n B_n^{(1)}}{Q_n} + w_0'''(0) \frac{D}{\rho\omega^2} \sum_{n=-2}^{\infty} \frac{B_n^{(3)}}{k_n Q_n} = i a_i k_0 \sum_{n=-2}^{\infty} \frac{B_n^{(0)}}{k_n Q_n}, \tag{59}$$

$$w_0'(0) \Big[\frac{J_0}{2\rho} + i \sum_{n=-2}^{\infty} \Big(P_n - \frac{D}{\rho\omega^2} k_n^2 \Big) \frac{k_n B_n^{(1)}}{Q_n} \Big] + w_0'''(0) \frac{iD}{\rho\omega^2} \sum_{n=-2}^{\infty} \Big(P_n - \frac{D}{\rho\omega^2} k_n^2 \Big) \frac{B_n^{(3)}}{k_n Q_n} =$$

$$- a_i k_0 \Big[i \frac{J_0}{2\rho} + \sum_{n=-2}^{\infty} \Big(P_n - \frac{D}{\rho\omega^2} k_n^2 \Big) \frac{B_n^{(0)}}{k_n Q_n} \Big]. \tag{60}$$

The solution $w_0'(0)$ and $w_0'''(0)$ of this system is substituted in (58), which finalises the calculations of the coefficients A_m^o in the odd component of the deflection.

In the important limiting case, where the rigid plate length under the ice plate is equal to the water depth, $L = H$, in (50) we have $P_m^{(G)} = 0$,

$$P_m = \frac{H^3}{q} \frac{\kappa_m^4 + \delta}{\kappa_m^2} \frac{1 - \cosh \kappa_m}{\cosh \kappa_m}, \qquad P_m^{(0)} = -\frac{H^3}{q} (\kappa_m^2 + \kappa_0^2),$$

and the series with u_k in the definitions of $B_n^{(0)}$, $B_n^{(1)}$, and $B_n^{(3)}$ should be removed. Then, the coefficients in the system (59) and (60) are readily calculated, which makes the solution of this limiting problem straightforward.

In another limiting case, where the rigid plate is only above the floating plate, $L = 0$, we use the limits (49), (50) but for the potential, $\phi_o(0, y) = 0$ for $-H < y < 0$. The calculations provide an account for (29),

$$A_m^o = -\frac{D w_o''(0)}{\rho\omega^2 Q_m}. \tag{61}$$

Equation (30), where now the integral is zero, and (61) give

$$2D w_o''(0) \Big[1 + i \frac{J_0}{2\rho} \sum_{n=-2}^{\infty} \frac{k_n}{Q_n} \Big] = -i a_i k_0 J_0 \omega^2, \tag{62}$$

which together with (61) explicitly define the coefficients A_m^o .

4. Numerical Algorithms

Calculations in this and the following sections are performed for a sea ice plate with ice density $\rho_{ice} = 917$ kg/m^3, thickness $h = 1$ m, Young's modulus $E = 4.2 \times 10^9$ N/m^2, and Poisson's ration $\nu = 0.33$, see [10,25]. The water density is 1025 kg/m^3, the water depth is $H = 10$ m, and the gravitational acceleration is $g = 9.8$ m/s^2. The rigid plate is made of the same ice, $\rho_r = \rho_{ice}$, with the plate length above the floating plate, $\ell = 1$ m, and the plate length below the floating plate L varies from 0 m to 10 m. The plate thickness h_r is 10 cm. Then, the mass of the vertical plate per unit width, $m_0 = \rho_r h_r (L + \ell)$, varies from 91.7 kg/m for $L = 0$ m to 1008.7 kg/m for $L = 10$ m. Correspondingly, the moment of inertia of the vertical plate per unit width, $J_0 = \frac{1}{3} m_0 (L^3 + \ell^3)/(L + \ell)$, varies from 30.6 kgm for $L = 0$ m

to 30,597.2 kg/m for $L = 10$ m. The ice rigidity D is equal approximately to 4×10^8 Nm. The characteristic length of the floating ice plate $L_c = (D/\rho g)^{\frac{1}{4}}$ is equal to 14.13 m, which is comparable with the water depth. Therefore, the finite depth of the water is important for the selected conditions.

The parameters $q = \rho\omega^2 H^5/D$ and $\delta = (\rho g - \rho_{ice} h\omega^2)H^4/D$ in the dispersion relation (1) written with respect to the dimensionless wavenumber $\kappa = kH$ read $(\kappa^4 + \delta)\kappa \tanh\kappa = q$ are related by the equation $\delta = a - bq$, where $a = (H/L_c)^4$ and $b = (\rho_{ice}h)/(\rho H)$. In the selected conditions, $a \approx 0.251$ and $b \approx 0.0895$. The parameter δ is positive for the wave frequencies such that $q < a/b$, where $a/b \approx 2.8$.

The ice deflection and the velocity of the flow are proportional to the incident wave amplitude a_i within the linear theory of hydroelasticity. We calculate the ice deflection for $a_i = 1$ m, bearing in mind that the deflections for other amplitudes are obtained by using a corresponding factor.

The period of the incident wave is assumed to be between 2 and 30 s, which corresponds to the wave frequency ω in the interval 0.21 $s^{-1} < \omega < 3.14$ s^{-1}. This interval provides $0 < q < 2.526$, and therefore $\delta > 0$. The dispersion relation (1) provides that this range of the wave frequencies corresponds to the range of the incident wave numbers $0.2133 < k_0 H < 1.2462$ and the incident wave length 50.43 m $< 2\pi/k_0 <$ 294.98 m. The roots of the dispersion relations are simple because $\delta > 0$ for the present conditions, see [8].

Note that the terms of the series (44) and (45) decay as $O(n^{-9})$, and the terms of the series (46) decay as $O(n^{-7})$ for $n \to \infty$. These series provide the even components of the plate deflection and strains in the plate. The series are evaluated numerically by direct summation. The series for the odd components of the solution decays slowly and care should be taken to evaluate these series with good accuracy.

4.1. Convergence Analysis for Odd Components of the Solution

The accuracy of the numerical solutions for the odd deflection and velocity potential depends on the number of terms M_o retained in the series (48) for the auxiliary function $u(y)$ and the number of pure imaginary roots of the dispersion relation N_o retained in the series (40) for $w_o(x)$ and $\phi_o(x, y)$. Then, the matrix in the algebraic system (56) is of size $M_o \times M_o$, and the values of each element of this matrix and of the right-hand side of the system are obtained by the summation of $N_o + 3$ terms.

The series for S_{kr}, see (56) converges slowly. The terms in this series are of order of $O(n^{-2})$ as $n \to \infty$. To find a reasonable value of N_o, which provides accurate numerical solution, we set $M_o = 20$ first and increase N_o starting from 100 with the step $\Delta N_o = 10$. The convergence of S_{kr} is demonstrated in Figure 2, where the maximum value, $S_{\max}$, of $|S_{kr}(N_0) - S_{kr}(N_0 - 10)|$ for $1 \le k, r \le M_0$ is shown as a function of N_0. The maxima are achieved at diagonal elements S_{kk}. Figure 2 shows that $N_o = 300$ provides the numerical values of S_{kr} with accuracy better than 10^{-5}. To ensure accuracy, $N_o = 500$ is used in our calculations.

It was shown that the accuracy of the solution depends mainly on N_o but not on M_0. The value of M_o affects the shape of $u(y)$ but has little influence on the deflection. $M_o = 20$ is used in the present calculations.

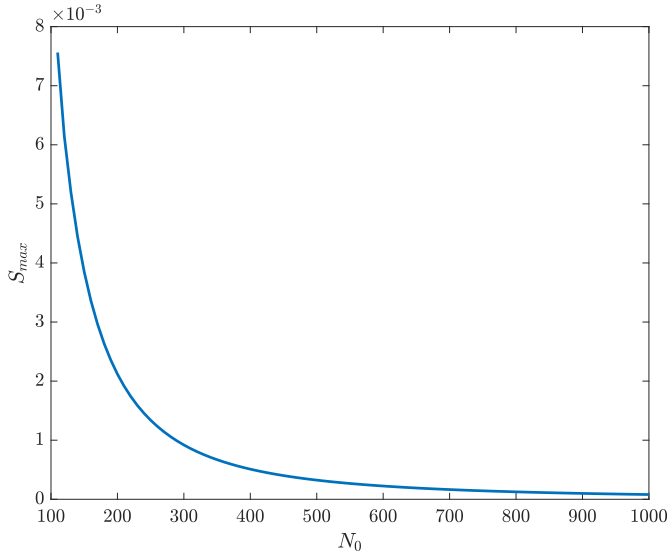

Figure 2. Convergence of the series S_{kr} with respect to N_o.

4.2. Roots of the Dispersion Relation

There is a single positive root of the dispersion equation, $(\kappa^4 + \delta)\kappa \tanh \kappa - q = 0$, because the left-hand side of this equation is negative at $\kappa = 0$, and it increases monotonically with the increase in κ. The real solution κ_0 is calculated by the bisection method, which narrows an interval that contains a root down to 1×10^{-14}. The pure imaginary roots of the dispersion relation, $\kappa_n = i\mu_n$, where $n \geq 1$, satisfy the equation

$$\tan \mu = -\frac{q}{\mu(\mu^4 + \delta)}, \tag{63}$$

where the right-hand side is negative for positive μ if $\delta > 0$ as in our conditions. The visual inspection of the sides of Equation (63) suggests that $\mu_n = \pi n - \sigma_n$, where σ_n is calculated by iterations,

$$\sigma_n^{(k+1)} = \arctan\left(\frac{q}{[\pi n - \sigma_n^{(k)}]([\pi n - \sigma_n^{(k)}]^4 + \delta)}\right), \tag{64}$$

with the initial guess $\sigma_n^{(0)} = 0$. Equation (64) shows that $\mu_n = \pi n - q(\pi n)^{-5} + O(n^{-6})$ as $n \to \infty$. This asymptotic formula is used to investigate, and improve if needed, convergence of the series from Section 3.

As to the complex roots, $\kappa_{-1} = a + ib$ and $\kappa_{-2} = -a + ib$, where $a > 0$ and $b > 0$, the values a and b are obtained by solving the system of two nonlinear equations,

$$a^5 - 10a^3b^2 + 5ab^4 + \delta a = q\frac{\sinh(2a)}{\cosh(2a) - \cos(2b)}, \tag{65}$$

$$5a^4b - 10a^2b^3 + b^5 + \delta b = -q\frac{\sin(2b)}{\cosh(2a) - \cos(2b)}, \tag{66}$$

by the Newton iteration method. Equations (65) and (66) yield that $b > a$ for $q > 0$. The asymptotic behaviors of κ_{-1} as $q \to 0$ were investigated in [9].

5. Numerical Results

In this section, the numerical results for the amplitudes of heave and pitch motions of the rigid plate, and the deflection of the ice plate and the strain in it, are presented. Calculations are performed for the parameters of the floating plate, the rigid plate, and the frequency range of the incident wave listed in Section 4. In the present study, only the length of the rigid plate in water L and the wavenumber of the incident wave k_0 vary. We use the corresponding dimensionless quantities $\tilde{L} = L/H$ and $\kappa_0 = k_0 H$ below.

5.1. Motions of the Rigid Elastic Plate

The complex amplitude of the vertical displacement of the rigid plate is given by (19) and (44),

$$\eta_a = \frac{a_i}{1-\gamma}, \tag{67}$$

where γ is defined in (44),

$$\gamma = \frac{im_0q^2}{\rho H^2}\sum_{n=-2}^{\infty}\frac{1}{\kappa_n(\kappa_n^4+\delta)^2\tilde{Q}_n}, \qquad \tilde{Q}_n = 1+q\frac{5\kappa_n^4+\delta-q}{(\kappa_n^4+\delta)^2\kappa_n^2}. \tag{68}$$

It is seen that $\eta_a = a_i$ if the mass of the rigid plate is negligible. Note that $\gamma \to 0$ as $q \to 0$, which is for long waves. In general, $\eta_a = |\eta_a|e^{i\delta_\eta}$, where δ_η is the phase shift of the heave response of the rigid plate. The dimensionless amplitude $|\eta_a|/a_i$ as a function of the dimensionless frequency $\sqrt{q} = \omega\sqrt{\rho H^5/D}$ is shown in Figures 3a,c for the different dimensionless length of the rigid plate, $\tilde{L} = L/H$, keeping all other parameters constant. The gap between the vertical rigid plate and the bottom is small in Figure 3c. These figures show that the amplitude of the heave motion of the vertical rigid plate is close to the amplitude of the incident wave a_i. The heave amplitude is slightly greater than a_i for long waves and smaller than a_i for short waves decreasing monotonically with the wave frequency. The length of the plate L increases its mass and, therefore, its inertia.

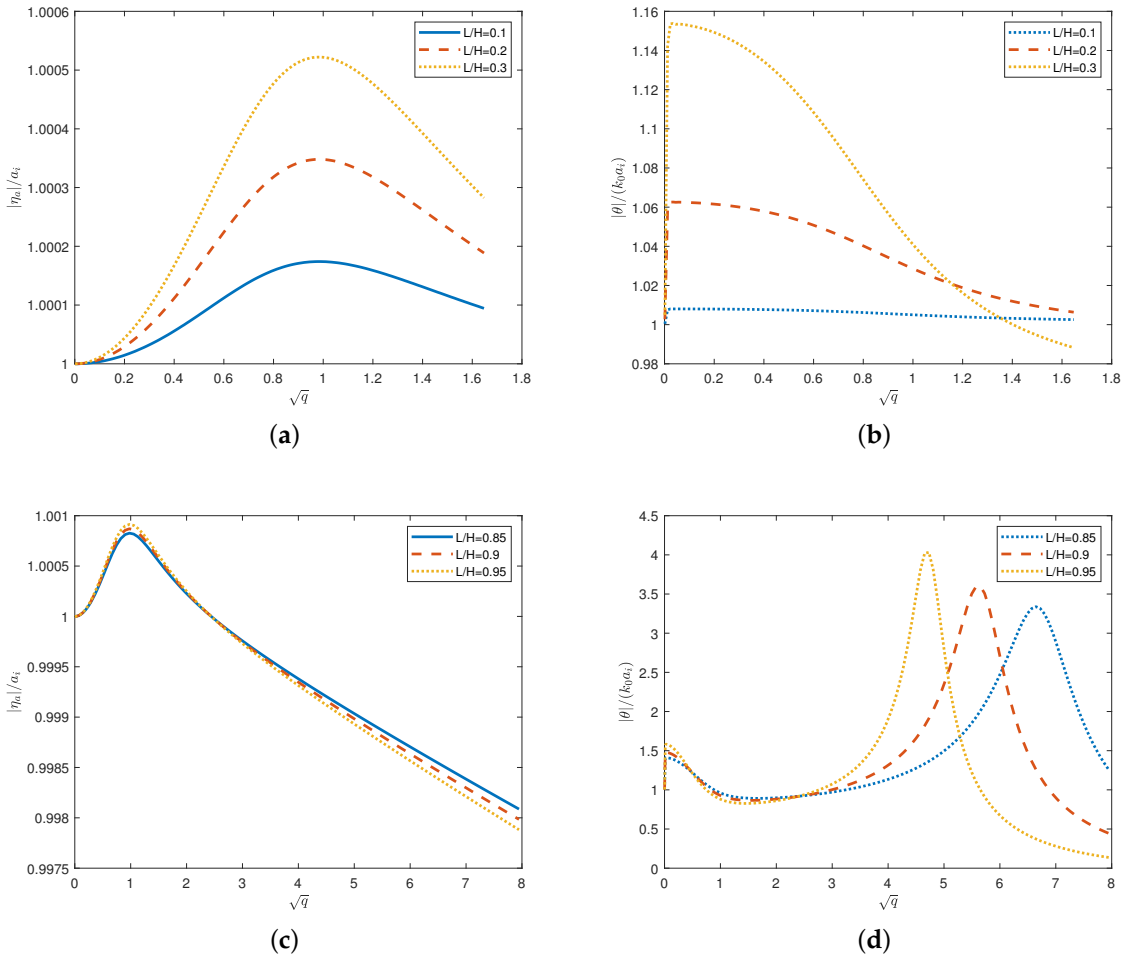

Figure 3. The dimensionless amplitudes of the heave (**a**,**c**), and pitch (**b**,**d**), motions of the rigid plate as functions of the dimensionless frequency $\sqrt{q}$ for different dimensionless length of the rigid plate $\tilde{L} = L/H$.

The complex amplitude of the rigid plate rotation is given by (19), $\theta_a = ik_0a_i + w_o'(0)$, where $w_o'(0)$ is the solution of the system (59) and (60). The scaled amplitude of the pitch motion, $|\theta_a|/(k_0a_i)$, is shown in Figures 3b,d as a function of the dimensionless frequency $\sqrt{q}$ for different dimensionless length of the rigid plate $\tilde{L}$. The pitch amplitude strongly depends on the wave frequency. The amplitude sharply increases for long waves, where $q \ll 1$, and then peaks at a certain value of $q_c(\tilde{L})$, which depends on the rigid plate length. Note that $q_c(\tilde{L})$ decreases with increase in $\tilde{L}$, see Figures 3d. The value $q_c(\tilde{L})$ can be estimated using the Equation (12), where the first term on the right-hand side, $M_s(0^+,t) - M_s(0^-,t)$, represents the restoring force proportional to the angle $\theta(t)$ approximately. The second term, $M_f(0^+,t) - M_f(0^-,t)$, represents the hydrodynamic moment acting on the oscillating rigid plate. This term contains the component $-J_a\theta''(t)$, where J_a is the added moment of inertia of the rigid plate. It is clear that J_a increases with increase in $\tilde{L}$. Therefore, the natural frequency of the system decreases with increase in $\tilde{L}$, which explains the shift of the peak frequency in Figure 3d. More details about the rigid plate motions in long waves, which is for small dimensionless frequency $\sqrt{q}$, are shown in Figures 4a,b.

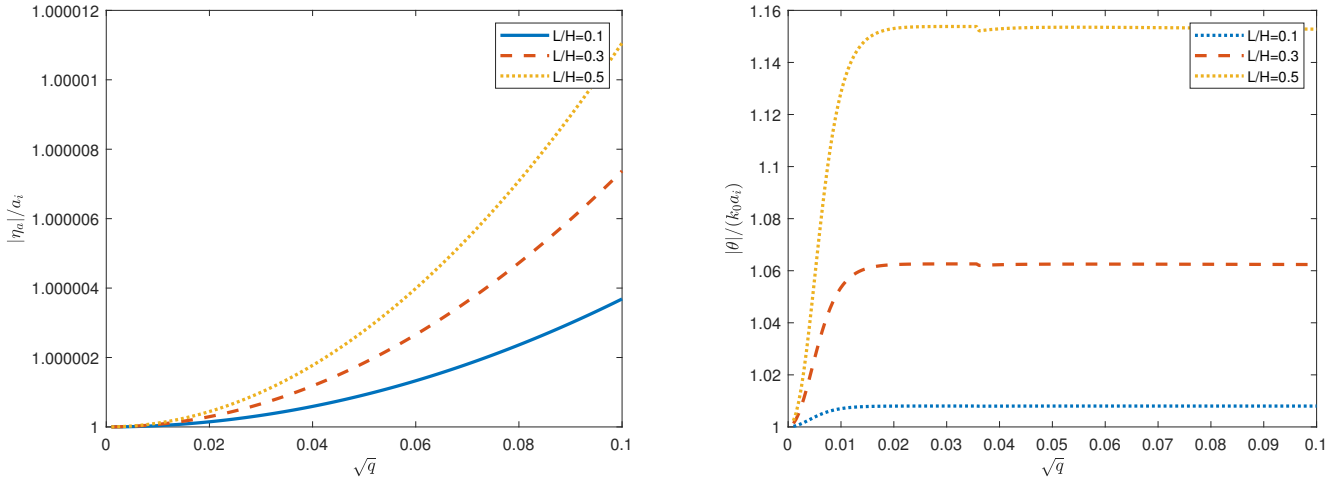

Figure 4. The dimensionless amplitudes of the heave (**a**) and pitch (**b**) motions of the rigid plate for small dimensionless frequency $\sqrt{q}$ and different length of the rigid plate $\tilde{L}$

5.2. Deflection of the Floating Ice Plate

The complex plate deflection $w(x)$ is given by (17), which provides

$$w(x) = w_{inc}(x) + w_o(x) + w_e(x) =$$

$$= \begin{cases} ae^{ik_0x} + \sum_{n=-2}^{N_e} A_n^e e^{ik_nx} + \sum_{n=-2}^{N_o} A_n^o e^{ik_nx} & (x \geq 0), \\ ae^{ik_0x} + \sum_{n=-2}^{N_e} A_n^e e^{-ik_nx} - \sum_{n=-2}^{N_o} A_n^o e^{-ik_nx} & (x < 0). \end{cases} \quad (69)$$

Here, $N_e = 10$ was used. The value of N_o was discussed in subsection 4.1.

The length of the rigid plate is the main parameter affecting reflection and transmission of incident waves. The dimensionless amplitude of the plate deflection, $|w(x)|/a_i$, is shown in Figure 5, where we set the incident wave frequency $\omega = 0.5\ \mathrm{s}^{-1}$ and vary the length of the rigid plate L. It can be seen that the length of the rigid plate does not change the pattern of the deflection curve but affects the amplitudes of reflection and transmission waves. The amplitude of the transmitted wave decreases, and the amplitude of the reflected wave increases with the increase in the length of the rigid plate.

The dimensionless amplitudes of the even, $|w_e(x)|/a_i$, and odd, $|w_o(x)|/a_i$, components of the plate deflection are shown in Figure 6 for different frequencies of the incident

wave ω and $\tilde{L} = 0.5$. It is seen that the odd component of the plate deflection, which is associated with the pitch motion of the rigid vertical plate, is much more important than the even component, which is associated with the heave motion of the rigid plate.

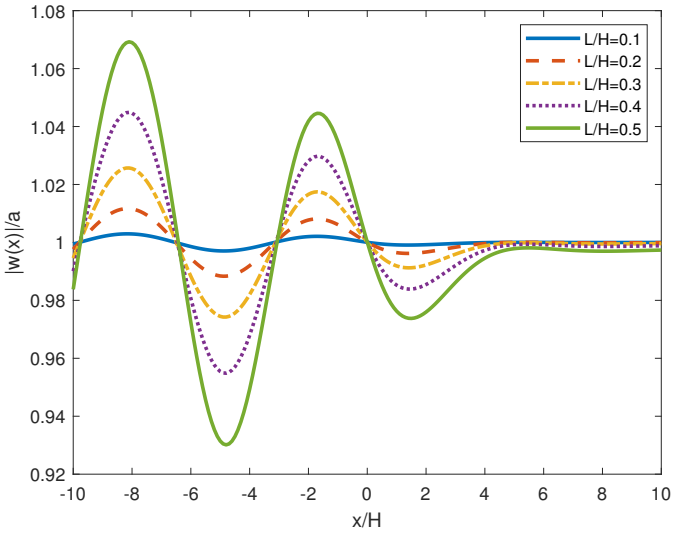

Figure 5. The dimensionless amplitudes of ice deflection for $\omega = 0.5\ \mathrm{s}^{-1}$ and different rigid plate length.

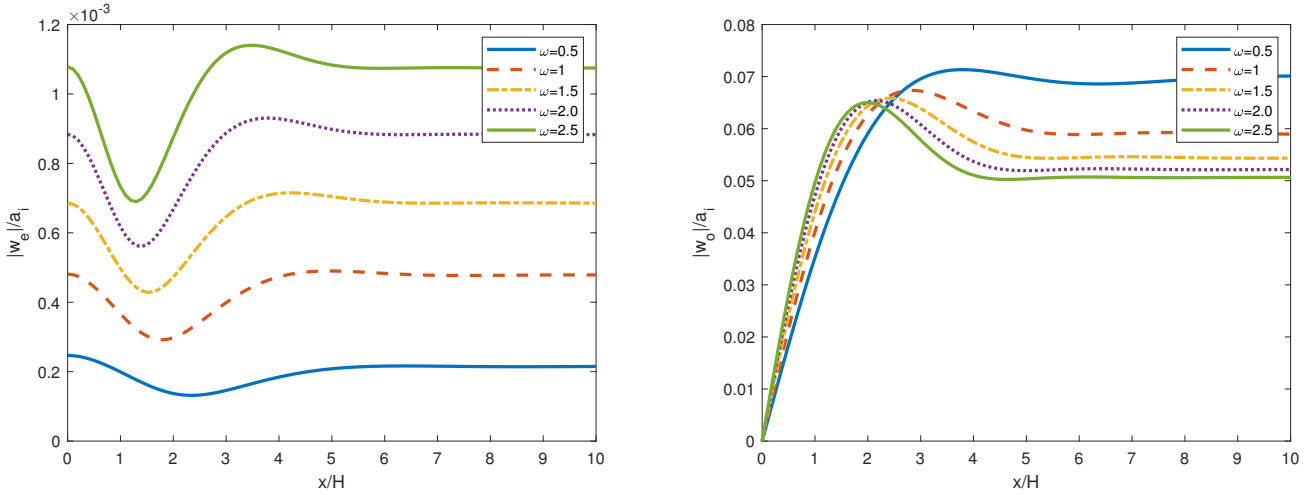

(**a**) (**b**)

Figure 6. The dimensionless amplitudes of the even (**a**), $|w_e(x)|/a_i$, and odd (**b**), $|w_o(x)|/a_i$, components of the plate deflection for different frequencies of the incident wave ω and $\tilde{L} = 0.5$. (**a**) Heave motion case. (**b**) Pitch motion case.

5.3. Strain Distribution in the Ice Plate

Similar to decomposition of the plate deflection (69), the complex strain in the plate, see (33), can be decomposed as

$$\varepsilon(x) = \varepsilon_{inc}(x) + \varepsilon_o(x) + \varepsilon_e, \tag{70}$$

where $\varepsilon_{inc}(x)$ is the complex strain in the incident wave,

$$\varepsilon_{inc}(x) = -\frac{1}{2} h a_i a_0^2 e^{ik_0 x}, \tag{71}$$

$\varepsilon_e(x)$ is the even strain component given by (46), and $\varepsilon_o(x)$ is the odd strain component.

$$\varepsilon_o(x) = \frac{1}{2}\frac{d^2 w_0}{dx^2} = -\frac{1}{2}h \sum_{n=-2}^{\infty} A_n^o k_n^2 e^{ik_0 x}, \tag{72}$$

see (33) and (40). The value $|\varepsilon_{inc}(x)|$ is taken as the strain scale ε_{sc}. The total strain amplitude, $|\varepsilon|(x)/\varepsilon_{sc}$, is shown in Figure 7a for different length of the rigid plate L and $\omega = 0.5\ \mathrm{s}^{-1}$. It is seen that the total strain is twice greater than the strain ε_{sc} in the incident wave just in front of the vertical rigid plate for the incident wave travelling from left to right and $L = H/2$. The even strain component, see Figure 7b, is much smaller than the odd component, see Figure 7c.

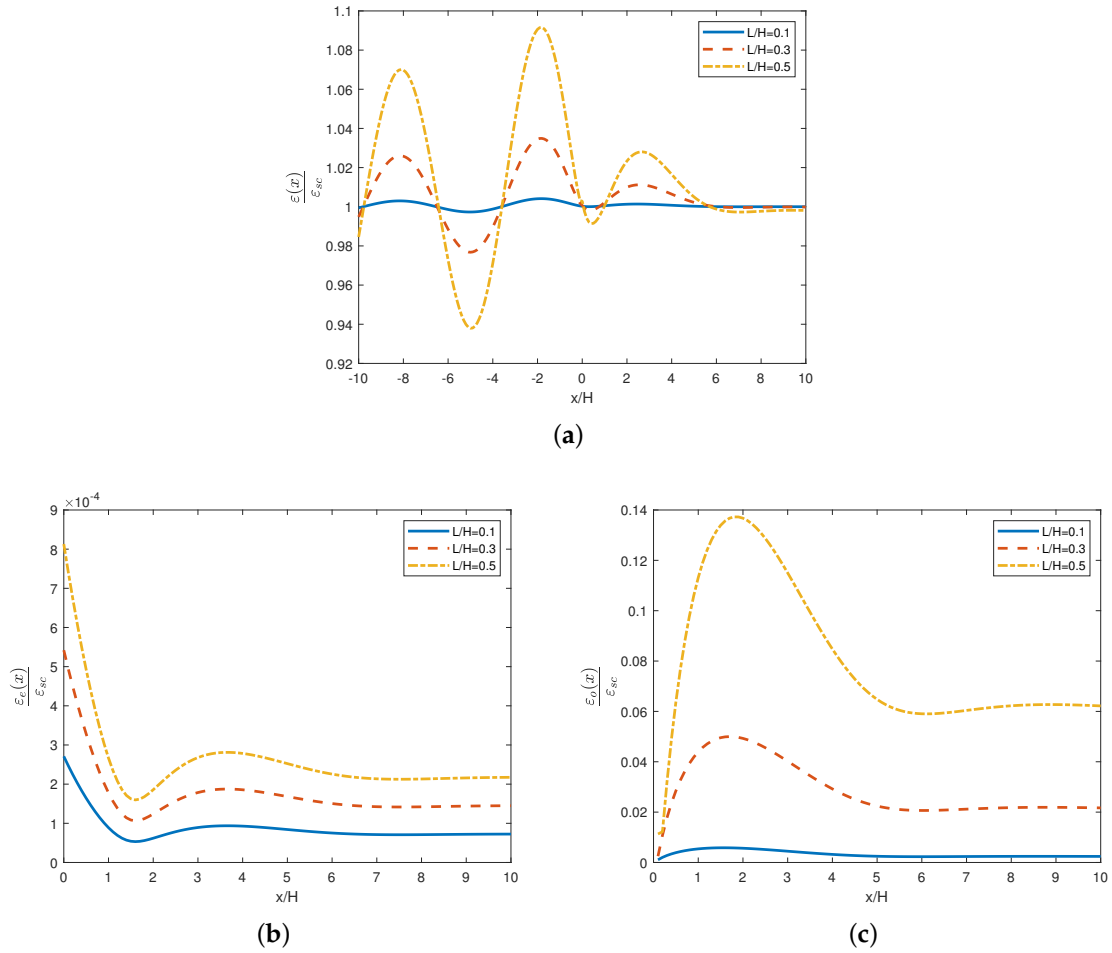

Figure 7. The scaled amplitudes of the total (**a**), even (**b**), $|\varepsilon_e(x)|/\varepsilon_{sc}$, and odd (c), $|\varepsilon_o(x)|/\varepsilon_{sc}$, components of the strain distribution in the floating plate for $\omega = 0.5\ \mathrm{s}^{-1}$ and different lengths of the rigid plate. (**a**) Total strain. (**b**) Even strain. (**c**) Odd strain.

6. Conclusions

The two-dimensional problem of interaction between an incident hydroelastic wave and a floating elastic ice plate with a rigid vertical plate built in it was studied within the linear theory of hydroelasticity. Due to the symmetry of the problem, the solution was decomposed into the sum of even and odd components, which represent the solution of the heave motion problem and the solution of the pitch motion problem for the rigid plate respectively. The vertical mode method was used to find the even and odd solutions. The even problem was solved analytically. The odd problem required one to satisfy mixed boundary conditions by the odd component of the velocity potential.

The numerical results for the motions of the rigid plate and the amplitude of ice plate deflection and strain were presented and discussed. The influence of the incident wave frequency and the length of the rigid plate on the floating plate response was investigated. It was revealed that the heave motion of the rigid plate much less affect the floating plate deflection than the pitch motion of the rigid plate. Longer rigid plates were shown to reflect more energy of the incident wave. The heave motion of the rigid plate decreases with increases of the frequency of the incident wave. Figures 6 and 7 indicate that the rotation of the rigid plate due to the incident wave is the main factor of increasing strains in the ice plate.

The obtained solutions will be used to investigate the strain distributions in the floating plate and the effect of the rigid plate on the magnitude of the strains in the plate. It is expected that the maximum strain is achieved in front of the rigid plate, see Figure 7, and can approach the yield strain leading to breaking of the floating plate in front of the rigid vertical plate. The problem with two and more vertical plates built in a floating elastic plate will be also studied. It is expected that trapped modes can be found for configurations with several plates.

Author Contributions: Conceptualization, Q.W. and T.K.; data curation, Q.W. and T.K.; methodology, T.K. and A.K.; software, Q.W. and T.K.; validation, Q.W., T.K. and B.N.; formal analysis, B.N. and A.K.; investigation, Q.W., T.K. and A.K.; resources, B.N.; writing—original draft preparation, Q.W., T.K. and A.K.; writing—review and editing, T.K. and A.K.; supervision, B.N.; project administration, B.N.; and funding acquisition, B.N. All authors have read and agreed to the published version of the manuscript.

Funding: This work is supported by the National Natural Science Foundation of China (Nos. 52192693, 52192690, 51979051, 51979056, and U20A20327), and the National Key Research and Development Program of China (2021YFC2803400), to which the authors are most grateful.

Institutional Review Board Statement: Not applicable.

Informed Consent Statement: Not applicable.

Data Availability Statement: Data are contained within the article.

Conflicts of Interest: The authors declare no conflict of interest.

Nomenclature

x	Horizontal coordinate
y	Vertical coordinate
t	Time
H	Water depth
ρ	Water density
g	Gravity acceleration
h	Ice plate thickness
ρ_{ice}	Ice density
E	Youngs modulus of ice
ν	Poissons ratio of ice
D	Ice rigidity
ℓ	Length of the rigid plate above the ice
L	Length of the rigid plate under the ice
h_r	Rigid plate thickness
m_0	Mass of the rigid plate
J_0	Moment of inertia of the rigid plate
a_i	Incident wave amplitude
ω	Incident wave frequency
k_0	Wave number of the incident wave
Φ	Total velocity potential
ϕ	Spatial velocity potential

ϕ_{inc}	Velocity potential of the incident wave
ϕ_e	Even component velocity potential
ϕ_o	Odd component velocity potential
W	Total ice deflection
w	Spatial ice deflection
w_{inc}	Ice deflection of incident wave
w_e	Even component ice deflection
w_o	Odd component ice deflection
P	Hydrodynamic pressure
θ	Inclination angle of the rigid plate
θ_a	Complex amplitude of rigid plate inclination angle
η	Vertical displacement of the rigid plate
η_a	Complex amplitude of rigid plate vertical displacement
N_s	Shear force in the ice plate
M_s	Bending moment in the ice plate
M_f	Hydrodynamic moments acting on the submerged part of the rigid plate
a_T	Amplitude of transmitted wave
δ_T	Phase of transmitted wave
a_R	Amplitude of reflected wave
δ_R	Phase of reflected wave
k	Wave number
κ	Dimensionless wave number, $\kappa = kH$
q	Dimensionless parameter in dimensionless dispersion relation
δ	Dimensionless parameter in dimensionless dispersion relation
$E(x,t)$	Time-periodic strains in the ice plate
ϵ	Amplitude of strains in the ice plate
$f_n(y)$	Vertical mode function
Q_n	Scalar product of vertical mode function
A_m^e	Unknown coefficients for even functions
A_m^o	Unknown coefficients for odd functions
ε_e	Strain for even ice deflection
$u(y)$	Unknown function
u_k	Coefficients of the unknown function
$\xi = (y+H)/(H-L)$	Stretched vertical coordinate variable
$T_{2k}(\zeta)$	Chebyshev polynomials of the first kind and degree $2k$

References

1. Gautier, D.L.; Bird, K.J.; Charpentier, R.R.; Grantz, A.; Houseknecht, D.W.; Klett, T.R.; Moore, T.E.; Pitman, J.K.; Schenk, C.J.; Schuenemeyer, J.H.; et al. Assessment of undiscovered oil and gas in the Arctic. *Science* **2009**, *324*, 1175–1179. [CrossRef]
2. Korobkin, A.A.; Părău, E.I.; Vanden-Broeck, J.M. The mathematical challenges and modelling of hydroelasticity. *Philos. Trans. R. Soc. Lond. A Math. Phys. Eng. Sci.* **2011**, *369*, 2803–2812. [CrossRef]
3. Smith, F.; Korobkin, A.A.; Părău, E.I.; Feltham, D.; Squire, V. Modelling of sea-ice phenomena. *Philos. Trans. R. Soc. Lond. A Math. Phys. Eng. Sci.* **2018**, *376*, 20180157. [CrossRef]
4. Lubbad, R.; Loset, S. A numerical model for real-time simulation of ship-ice interaction. *Cold Reg. Sci. Technol.* **2011**, *65*, 111–127. [CrossRef]
5. Jeon, S.K.; Kim, Y.I. Numerical simulation of level ice–structure interaction using damage-based erosion model. *Ocean Eng.* **2021**, *220*, 108485. [CrossRef]
6. Truong, D.D.; Jang, B.S. Estimation of ice loads on offshore structures using simulations of level ice-structure collisions with an influence coefficient method. *Appl. Ocean Res.* **2022**, *125*, 103235. [CrossRef]
7. Squire, V.; Hosking, R.J.; Kerr, A.D.; Langhorne, P. *Moving Loads on Ice Plates*; Kluwer: Dordrecht, The Netherlands, 1996.
8. Korobkin, A.A.; Malenica, S.; Khabakhpasheva, T.I. Interaction of flexural-gravity waves in ice cover with vertical walls. *Philos. Trans. R. Soc. Lond. A Math. Phys. Eng. Sci.* **2018**, *376*, 20170347. [CrossRef] [PubMed]
9. Korobkin, A.A.; Malenica, S.; Khabakhpasheva, T.I. The vertical mode method in the problems of flexural-gravity waves diffracted by a vertical cylinder. *Appl. Ocean Res.* **2019**, *84*, 111–121. [CrossRef]

10. Brocklehurst, P.; Korobkin, A.A.; Părău, E.I. Hydroelastic wave diffraction by a vertical cylinder *Philos. Trans. R. Soc. Lond. A Math. Phys. Eng. Sci.* **2011**, *369*, 2832–2851.
11. Disibuyuk, N.B.; Yilmaz, O.; Korobkin, A.A.; Khabakhpasheva, T.I. An Iterative Method for Interaction of Hydro-Elastic Waves with Several Vertical Cylinders of Circular Cross-Sections. *J. Mar. Sci. Eng.* **2022**, *10*, 723. [CrossRef]
12. Disibuyuk, N.B.; Korobkin, A.A.; Yilmaz, O. Diffraction of flexural-gravity waves by a vertical cylinder of non-circular cross section. *Appl. Ocean Res.* **2020**, *101*, 102234. [CrossRef]
13. Zeng, L.D.; Korobkin, A.A.; Ni, B.Y.; Xue, Y.Z. Moving load in an ice channel with a crack. *Appl. Ocean Res.* **2022**, *121*, 103086. [CrossRef]
14. Zeng, L.D.; Korobkin, A.A.; Ni, B.Y.; Xue, Y.Z. Flexural-gravity waves in ice channel with a lead. *JFM* **2021**, *921*, A10. [CrossRef]
15. Xue, Y.Z.; Zeng, L.D.; Ni, B.Y.; Korobkin, A.A.; Khabakhpasheva, T.I. Hydroelastic response of an ice sheet with a lead to a moving load. *PoF* **2021**, *33*, 037109. [CrossRef]
16. Shishmarev, K.A.; Khabakhpasheva, T.I.; Korobkin, A.A. The response of ice cover to a load moving along a frozen channel. *Appl. Ocean Res.* **2016**, *59*, 313–326. [CrossRef]
17. Korobkin, A.A.; Khabakhpasheva, T.I.; Papin, A.A. Waves propagating along a channel with ice cover. *Eur. J. Appl. Math.-B/Fluids* **2014**, *47*, 166–175. [CrossRef]
18. Gunasundari, C.; Ashok, R.; Manam, S.R. Effect of a Pressure Ridge on Ice-Coupled Gravity Waves. *Int. J. Offshore Polar Eng.* **2022**, *32*, 313–320. [CrossRef]
19. Khabakhpasheva, T.I.; Korobkin, A.A. Hydroelastic behavior of compound floating plate in waves. *J. Eng. Math.* **2002**, *44*, 21–40. [CrossRef]
20. Korobkin, A.A.; Khabakhpasheva, T.I. Plane linear problem of the immersion of an elastic plate in an ideal incompressible fluid. *J. Appl. Mech. Tech. Phys.* **1999**, *40*, 491–500. [CrossRef]
21. Lawrie, J.B.; Abrahams, I.D. An orthogonality relation for a class of problems with high-order boundary conditions; applications in sound-structure interaction. *Quart. J. Mech. Appl. Math.* **1999**, *52*, 161–181. [CrossRef]
22. Lawrie, J.B.; Abrahams, I.D. On the propagation and scattering of fluid-structural waves in a three-dimensional duct bounded by thin elastic walls. In Proceedings of the Symposium IUTAM on Diffraction and Scattering in Fluid Mechanics and Elasticity, Manchester, UK, 16–20 July 2000; pp. 279–288.
23. Manam, S.R.; Bhattacharjee, J.; Sahoo, T. Expansion formulae in wave structure interaction problems. *Proc. R. Soc. A Math. Phys. Eng. Sci.* **2006**, *462*, 263–287. [CrossRef]
24. Mandal, S.; Sahoo, T.; Chakrabarti, A. A note on convergence of expansion formula for wave structure interaction problems. In Proceedings of the 30th Internatinal Workshop on the Water Waves and Floating Bodies, Bristol, UK, 12–15 April 2015.
25. Squire, V.; Robinson, W; Langhorne, P.; Haskell, T. Vehicles and aircraft on floating ice. *Nature* **1988** 333, 159–161 [CrossRef]